# Precise equilibrium structure of thiazole $(c-C_3H_3NS)$ from twenty-four isotopologues

Cite as: J. Chem. Phys. 155, 054302 (2021); doi: 10.1063/5.0057221

Submitted: 18 May 2021 • Accepted: 30 June 2021 •

**Published Online: 3 August 2021** 







Brian J. Esselman, D. Maria A. Zdanovskaia, D. Andrew N. Owen, D. John F. Stanton, Landon, D. Stanton, R. Claude Woods, 1,a) and Robert J. McMahon 1,a)

## **AFFILIATIONS**

- Department of Chemistry, University of Wisconsin-Madison, 1101 University Avenue, Madison, Wisconsin 53706-1322, USA
- Quantum Theory Project, Departments of Physics and Chemistry, University of Florida, Gainesville, Florida 32611, USA
- a) Authors to whom correspondence should be addressed: johnstanton@chem.ufl.edu; rcwoods@wisc.edu; and robert.mcmahon@wisc.edu

## **ABSTRACT**

The pure rotational spectrum of thiazole (c-C<sub>3</sub>H<sub>3</sub>NS, C<sub>5</sub>) has been studied in the millimeter-wave region from 130 to 375 GHz. Nearly 4800 newly measured rotational transitions for the ground vibrational state of the main isotopologue were combined with previously reported measurements and least-squares fit to a complete sextic Hamiltonian. Transitions for six singly substituted heavy-atom isotopologues (13C, 15N, 33S, 34S) were observed at natural abundance and likewise fit. Several deuterium-enriched samples were prepared, which gave access to the rotational spectra of 16 additional isotopologues, 14 of which had not been previously studied. The rotational spectra of each isotopologue were fit to A- and S-reduced distorted-rotor Hamiltonians in the I<sup>r</sup> representation. The experimental values of the ground-state rotational constants  $(A_0, B_0, \text{ and } C_0)$  from each isotopologue were converted to determinable constants  $(A_0'', B_0'', \text{ and } C_0'')$ , which were corrected for effects of vibration-rotation interactions and electron-mass distributions using coupled-cluster singles, doubles, and perturbative triples calculations [CCSD(T)/cc-pCVTZ]. The moments of inertia from the resulting constants ( $A_e$ ,  $B_e$ , and  $C_e$ ) of 24 isotopologues were used to determine the precise semi-experimental equilibrium structure ( $r_e^{SE}$ ) of thiazole. As a basis for comparison, a purely theoretical equilibrium structure was estimated by an electronic structure calculation [CCSD(T)/cc-pCV5Z] that was subsequently corrected for extrapolation to the complete basis set, electron correlation beyond CCSD(T), relativistic effects, and the diagonal Born-Oppenheimer correction. The precise re structure is compared to the resulting "best theoretical estimate" structure. Some, but not all, of the best theoretical  $r_e$  structural parameters fall within the narrow statistical limits (2 $\sigma$ ) of the  $r_e^{\text{SE}}$  results. The possible origin of the discrepancies between the best theoretical estimate  $r_e$ and semi-empirical  $r_e^{\text{SE}}$  structures is discussed.

Published under an exclusive license by AIP Publishing. https://doi.org/10.1063/5.0057221

## INTRODUCTION

The aromatic heterocycle, thiazole (c-C<sub>3</sub>H<sub>3</sub>NS, Fig. 1), is an important molecule in chemistry and biology. In N-alkylated form, thiazole is a component of thiamine (vitamin B<sub>1</sub>) and is the source of unique reactivity that occurs at C2, the position between nitrogen and sulfur. This reactivity forms the basis of many critical functions in nature and has also been exploited in synthetic chemistry.<sup>2</sup> The thiazole structure is found in pharmaceuticals, including penicillin and many others.<sup>2</sup> Our own interest in thiazole derives from both structural and spectroscopic considerations. A detailed understanding of the molecular structure provides important context for understanding the chemical reactivity of thiazole. Its pure rotational spectrum is of considerable interest in

the context of recent developments in astrochemistry concerning the direct detection of aromatic compounds in interstellar space by radioastronomy.3-5 A few sulfur-containing molecules have been detected in the interstellar medium,<sup>6</sup> but none are representative of the organosulfur chemistry that is characteristic of terrestrial chemistry or biology. To us, the polar heterocyclic aromatic compounds thiophene (C<sub>4</sub>H<sub>4</sub>S) and thiazole (C<sub>3</sub>H<sub>3</sub>NS) represent important targets for radioastronomy, thereby motivating interest in their laboratory spectroscopy.

Thiazole ( $C_3H_3NS$ ,  $C_s$ ) is a slightly prolate ( $\kappa = -0.166$ ) asymmetric top (Fig. 1) with moderate and comparable dipole moment components along both its a- and b-principal axes [ $\mu_a$  = 1.286 (20) D,  $\mu_b = 0.966$  (20) D]. The rotational spectrum was first investigated from 16 to 30 GHz, resulting in the determination of its

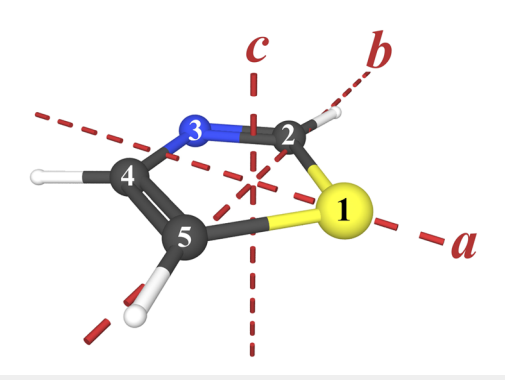


**FIG. 1.** Thiazole [c-C<sub>3</sub>H<sub>3</sub>NS,  $C_8$ ,  $\mu_a = 1.286$  (20) D,  $\mu_b = 0.966$  (20) D,  $\kappa = -0.166$ ] with principal axes and atom numbering.

rotational constants and the dipole moment components by the Stark effect.<sup>7</sup> The rotational constants from its main isotopologue and each of its singly substituted isotopologues were used to determine a substitution structure  $(r_s)$  using the Kraitchman analysis<sup>8</sup> with deuterium-enriched samples provided from previous syntheses.<sup>9-11</sup> Four atoms [C2, C5, H(C2), and H(C5)] are sufficiently close (<0.05 Å) to the *b*-principal axis that obtaining accurate results from this method of structure determination proved challenging. An attempt was made to improve the substitution structure by employing the center-of-mass condition, fixing the a-coordinate of H(C2), and iteratively adjusting the related parameters.8 This strategy resulted in an  $r_s$  structure with parameters consistent with those of other aromatic heterocycles and sulfur-containing compounds.

Several additional microwave transitions of thiazole in the 26.5-40 GHz frequency region were measured in a survey of rotational spectra for sulfur-containing compounds.<sup>12</sup> Subsequently, new transitions from 8 to 36 GHz and the rotational Zeeman effect were measured.<sup>13</sup> Using hyperfine-resolved, Fouriertransform microwave (FTMW) measurements, the rotational and nuclear quadrupole constants of the main isotopologue and its [34S]and [33S]-isotopologues were reported.14 The work of Kretschmer and Dreizler included the first determination of the quartic centrifugal distortion constants, in the van Eijck definition. 15 The rotational constants of the ground state and nine vibrationally excited states were determined from high-resolution IR spectra between 600 and 1400 cm<sup>-1</sup> by Hegelund et al. 16 The ground-state rotational constants were determined via simultaneous fitting of highresolution IR data for eight fundamentals and 12 microwave transitions from Bak et al.7 While the high-resolution IR work did not take advantage of additional rotational transitions reported since the original microwave work, 12-14 it did result in a well-determined set of A reduction quartic distortion constants in both I<sup>r</sup> and III<sup>r</sup> representations.

Two improved structure determinations have been reported since the original structure of Nygaard et al.:8 a combined microwave and gas-phase electron-diffraction structure  $(r_z)^{17}$  and a density functional theory (DFT)-based semi-experimental equilibrium structure  $(r_e^{SE})$ . Both of these updated structures relied upon the previously reported isotopologue rotational constants of Nygaard et al.8 and did not include updated spectroscopic constants

or additional isotopologues based on work subsequent to that of Nygaard et al. 12-14 To update the semi-experimental equilibrium structure of thiazole and the spectroscopic analysis of the isotopologues, we obtained and analyzed the rotational spectra of 24 thiazole isotopologues (14 of which have not been previously reported). With the exception of  $[4-^2H]$ -thiazole, the precision of rotational constants for all previously observed isotopologues was improved. These new data result in a highly precise semi-experimental equilibrium structure determination, which includes data from multiple isotopic substitutions of all atoms.

## **EXPERIMENTAL METHODS**

Thiazole was purchased commercially and used without further purification. Using a millimeter-wave spectrometer that has been described previously, 19,20 the rotational spectra of this sample and several isotopically substituted samples of thiazole described below were collected from 130-230 to 235-375 GHz in a continuous flow at room temperature with a sample pressure of 3 mTorr. The separate spectral segments were combined into a single broadband spectrum using Kisiel's Assignment and Analysis of Broadband Spectra (AABS) software, <sup>21,22</sup> and the ASROT/ASFIT, PLANM, and AC programs were employed for least-squares fitting and spectroscopic analysis.<sup>23</sup> A uniform frequency measurement uncertainty of 50 kHz was assumed for all new measurements, while the quoted measurement uncertainties were used for all previously published data.

## **COMPUTATIONAL METHODS**

Electronic structure calculations using coupled-cluster theory were carried out with a development version of the CFOUR program.<sup>24</sup> Optimized geometries were determined using analytic gradients. Coupled-cluster with singles, doubles, and perturbative triples [CCSD(T)] calculations were performed with the cc-pCVXZ (X = D, T, Q, 5) basis sets and include correlation of all electrons. Anharmonic vibrational frequencies and vibration-rotation interaction constants  $(\alpha_i)$  were determined using a VPT2 calculation at the CCSD(T)/cc-pCVTZ level of theory by calculating cubic and quartic force constants using second derivatives at displaced points. Magnetic calculations were performed to obtain the CCSD(T)/ccpCVTZ electron-mass corrections to the rotational constants. Corrections to the computed equilibrium structure were calculated following the method prescribed in the work of Heim et al. 25 The xrefit module of CFOUR was utilized to obtain the least-squares fit re structure. An iterative approach to the implementation of the structure fitting program, xrefit, has been automated in our program, xrefiteration. This program, which is useful in analyzing datasets involving a large number of isotopologues, will be described separately.<sup>26</sup> The output summary from *xrefiteration* is provided in the supplementary material.

Density functional theory computations were performed at the B3LYP/6-311+G(2d,p) level of theory using Gaussian  $16^{27}$  with the WebMO user interface.<sup>28</sup> B3LYP calculations relevant to solution phase isotopic enrichment included implicit solvation using a polarized continuum model. Computational output files, summaries of electronic structure calculations, and analyses can be found in the supplementary material.

## SYNTHESIS OF DEUTERIO THIAZOLES

Deuterium-containing samples of thiazole were prepared using acid- and base-catalyzed exchange reactions with  $D_2O$  (Scheme 1). Base-catalyzed H/D exchange was carried out using sodium carbonate under two different sets of conditions, resulting in product mixtures rich in  $[2^{-2}H]$ -thiazole [Scheme 1(a)] and  $[2,5^{-2}H]$ -thiazole [Scheme 1(b)]. Was based upon previous syntheses of  $[2^{-2}H]$ -thiazole using deuterated acetic acid and  $[2,4,5^{-2}H]$ -thiazole using  $D_2SO_4$ , well as upon our previous studies involving deuterium incorporation in thiophene. Each of these three synthetic procedures enabled the observation of rotational spectra of multiple thiazole isotopologues in a single broadband spectrum. The experimental procedures and mass spectra used for product characterization are provided in the supplementary material.

Under both basic and acidic conditions, H/D exchange at the 2-position is relatively facile, resulting in product mixtures rich in  $[2^{-2}H]$ -thiazole. Under acidic conditions, this preference for deuteriation is consistent with previous reports for thiazole. 8.11,30 While the 5-position is activated to electrophilic aromatic substitution (EAS) reactions,  $^{32,33}$  the H/D exchange under acidic conditions follows an addition–elimination mechanism due to the presence of the basic nitrogen atom in thiazole.  $^{34-36}$  Under basic conditions, H/D exchange at the 2-position is consistent with previous examples using strong bases, such as alkyl lithium reagents.  $^{34,37}$  Clearly, the rate of H/D exchange is slowest at the 4-position and the  $[2,4,5^{-2}H]$ -thiazole isotopologue is generated only in small amount. Given the relative rates of isotopic exchange, the methods in Scheme 1 are not amenable to the preparation of the  $[4^{-2}H]$ -,  $[2,4^{-2}H]$ -, or  $[4,5^{-2}H]$ -thiazole isotopologues.

The regioselectivity of the base-catalyzed H/D exchange can be rationalized by comparing the relative energies of the three regioisomeric deprotonated thiazoles ( $C_3H_2NS^-$ ). As shown in Fig. 2, there is a slight energetic preference of 0.5 kcal/mol for the 2-thiazole anion over the 5-thiazole anion [B3LYP/6-311+G(2d,p) with the polarized continuum model for water as a solvent]. This finding is qualitatively consistent with experimental observation in this and previous works. <sup>34,37,38</sup> In the sample generated using the

(a) 
$$N = \frac{Na_2CO_3}{D_2O, RT, 8 \text{ days}}$$
  $N = \frac{Na_2CO_3}{N}$   $N = \frac$ 

**SCHEME 1.** Base- and acid-catalyzed reactions for H/D exchange with thiazole.

(a) 
$$H \xrightarrow{\dot{S}} H \xrightarrow{-H^+} \bigoplus_{\dot{N}} H \xrightarrow{\dot{N}} H \xrightarrow{\dot{N}} \bigoplus_{\dot{N}} \bigoplus_{\dot{N}} H \xrightarrow{\dot{N}} \bigoplus_{\dot{N}} \bigoplus_{\dot{N}} H \xrightarrow{\dot{N}} \bigoplus_{\dot{N}} \bigoplus_{\dot{N}} H \xrightarrow{\dot{N}} \bigoplus_{\dot{N}} \bigoplus_{\dot{N}} \bigoplus_{\dot{N}} H \xrightarrow{\dot{N}} \bigoplus_{\dot{N}} \bigoplus_{\dot{N}} \bigoplus_{\dot{N}} \bigoplus_{\dot{N}} H \xrightarrow{\dot{N}} \bigoplus_{\dot{N}} \bigoplus_$$

**FIG. 2.** Relative energies of (a) deprotonated and (b) zwitterionic thiazole regioisomers. Energies calculated at B3LYP/6-311+G(2d,p) with the polarized continuum model for water as a solvent.

conditions in Scheme 1(a), the rotational transitions of  $[2^{-2}H]$ -thiazole were more than 50 times stronger than the transitions of  $[5^{-2}H]$ -thiazole. As the reaction temperature increased [Scheme 1(b)], the rapid production of both  $[2^{-2}H]$ - and  $[5^{-2}H]$ -thiazole converges to yield  $[2,5^{-2}H]$ -thiazole as the major product. The 4-thiazole anion is much higher in energy than its two regioisomers, which corresponds to a very low level of H/D exchange at that position, observed in this work and previously reported.

Interestingly, the same stabilization of a negative charge at the 2-position controls the regiochemical outcome of H/D exchange in both acidic and basic solutions. Due to the much greater basicity of the nitrogen atom in thiazole compared to the carbon atoms, the nitrogen is protonated, followed by carbon deprotonation, forming a zwitterion [Fig. 2(b)]. The same preference of C2 to hold negative charge under basic conditions leads to the stabilization of the corresponding zwitterion (by over 11 kcal/mol) relative to both its regioisomers. Accordingly, previously reported acidic H/D exchange  $^{30,35,38}$  and our acid-catalyzed reaction [Scheme 1(c)] generated predominantly [ $2^{-2}$ H]-thiazole.

## **ANALYSIS OF ROTATIONAL SPECTRA**

## Normal isotopologue

Spectroscopic constants for the ground vibrational state of the normal isotopologue of thiazole have recently been refined on the basis of data from both pure rotational spectroscopy and rotationally resolved infrared spectroscopy.<sup>29</sup> Key data pertinent to the current study are summarized in Table I. Spectroscopic constants are reported for A- and S-reduced, sextic Hamiltonians in the I<sup>r</sup> representation. The I<sup>r</sup> representation was chosen because of the slightly prolate nature of the normal isotopologue. The lowest-energy vibrationally excited state has an energy of 468 cm<sup>-1</sup>,<sup>39</sup> resulting in an intensity approximately one tenth that of the ground state at room temperature. The sparsity of the rotational spectrum of thiazole, with well-separated bands and a lack of intense transitions from vibrationally excited states, is advantageous to the current work involving

**TABLE I.** Spectroscopic constants for the ground vibrational state, normal isotopologue of thiazole (A- and S-reduced Hamiltonians, I<sup>r</sup> representation).<sup>a</sup>

	A reduction		S reduction
$A_0^{(A)}$ (MHz)	8 529.447 921(42)	$A_0^{(S)}$ (MHz)	8 529.448 627(42)
$B_0^{(A)}$ (MHz)	5 505.779 360(31)	$B_0^{(S)}$ (MHz)	5 505.776 921(31)
$C_0^{(A)}$ (MHz)	3 344.301 222(36)	$C_0^{(S)}$ (MHz)	3 344.303 097(36)
$\Delta_J$ (kHz)	0.912 608(17)	$D_J$ (kHz)	0.770 791(16)
$\Delta_{JK}$ (kHz)	-0.208669(34)	$D_{JK}$ (kHz)	0.642229(24)
$\Delta_K$ (kHz)	2.535 179(41)	$D_K$ (kHz)	1.826 097(39)
$\delta_J$ (kHz)	0.333 549 4(48)	$d_1$ (kHz)	-0.3335484(48)
$\delta_K$ (kHz)	1.077 224(32)	$d_2$ (kHz)	-0.0709086(21)
$\Phi_J$ (Hz)	0.0003070(30)	$H_J$ (Hz)	0.000 233 8(24)
$\Phi_{JK}$ (Hz)	-0.001270(17)	$H_{JK}$ (Hz)	-0.0022536(44)
$\Phi_{KI}$ (Hz)	-0.001611(35)	$H_{KI}$ (Hz)	0.0027678(97)
$\Phi_K$ (Hz)	0.004 277(23)	$H_K$ (Hz)	0.000 952(14)
$\phi_I$ (Hz)	0.0001570(10)	$h_1$ (Hz)	0.000 133 50(95)
$\phi_{JK}$ (Hz)	-0.000240(11)	$h_2$ (Hz)	0.000 036 65 (68)
$\phi_K$ (Hz)	0.003 851(22)	$h_3$ (Hz)	0.000 023 35(13)
$N_{ m lines}^{b}$	4 782	$N_{ m lines}^{b}$	4 782
$\sigma_{\rm fit}$ (MHz)	0.029	$\sigma_{\rm fit}$ (MHz)	0.029
$\kappa^{c}$	-0.166	$\kappa^{c}$	-0.166
$\Delta_i (\mu \mathring{A}^2)^d$	0.074754(2)	$\Delta_i (\mu \text{Å}^2)^{\text{d}}$	0.074633(2)

<sup>&</sup>lt;sup>a</sup>These values vary slightly from those in Ref. 29, which are determined by a combined dataset of IR and rotational data. Deviations are much smaller than the statistical uncertainty of each value.

structure determination. The sparse nature of the spectrum made it straightforward to identify and assign transitions for the naturally occurring heavy-atom isotopologues and minimized the spectral confusion in the analysis of mixed isotopologue samples.

## Thiazole isotopologues

Spectroscopic constants for a total of 23 additional isotopologues were obtained from a commercial sample and several deuteriated samples (Table II). The S reduction constants in the I<sup>r</sup> representation are provided below; the A reduction constants are available in the supplementary material. Centrifugal distortion constants that could not be adequately determined from the experimental data were held constant at their predicted values. Datasets with more than ~1500 transitions were sufficient to determine a full set of quartic and sextic constants, while datasets with fewer than ~200 transitions were insufficient to determine even a full set of quartic centrifugal distortion constants. Additional information concerning spectroscopic constants, least-squares fits, and data distribution plots are provided in the supplementary material.

The rotational spectrum of commercial thiazole provided six single-atom substitution isotopologues ( $^{13}$ C,  $^{15}$ N,  $^{33}$ S,  $^{34}$ S) at natural abundance, including substitution of each heavy-atom position of the ring. Although several of these isotopologues have been studied previously,  $^{8,14}$  the transition frequencies for most are not available and therefore could not be included in the current least-squares fits.

Six hyperfine-resolved, microwave transitions are available for [33S]-thiazole<sup>14</sup> and are included in the least-squares fits.

Deuteriated samples were generated (Scheme 1) with the dual purposes of updating the spectroscopic constants of the known, mono-substituted isotopologues of thiazole ( $[2^{-2}H]$ ,  $[4^{-2}H]$ , and  $[5^{-2}H]$ ) and identifying new, multiply substituted isotopologues. Initial searches for rotational transitions of new isotopologues were conducted using the estimated values of the spectroscopic constants. Specifically, the rotational constants for the normal isotopologue and the desired isotopologue were computed using CFOUR. Predicted constants for the desired isotopologue were adjusted by the same amount as the difference between the experimental and computational values of the main isotopologue. The estimated rotational constants, along with the centrifugal distortion constants from the most similar isotopologue, were used to predict the rotational transitions for the isotopologue of interest. This simple method was successful for identifying the transitions of several deuteriated isotopologues.

Due to the relative ease of generating enriched samples of [2–²H]-thiazole, over 4000 transitions were measured and least-squares fit for this isotopologue, resulting in a full set of quartic and sextic centrifugal distortion constants. These samples were sufficiently rich in [2–²H]-thiazole that the <sup>13</sup>C-, <sup>15</sup>N-, <sup>33</sup>S-, and <sup>34</sup>S-substituted isotopologues of [2–²H]-thiazole could also be observed and their spectroscopic constants determined. Decreasing numbers of transitions were least-squares fit for each of the heavy-atom

<sup>&</sup>lt;sup>b</sup>Number of independent transitions.

 $<sup>^{</sup>c}\kappa = (2B - A - C)/(A - C).$ 

<sup>&</sup>lt;sup>d</sup>Inertial defect ( $\Delta_i = I_c - I_a - I_b$ ) calculated with PLANM.

isotopologues based upon their decreasing natural abundance, resulting in the determination of fewer spectroscopic constants. Where particular spectroscopic constants could not be adequately determined, their values were held constant at the computed values.

Under mildly basic reaction conditions, thiazole H/D exchange occurred at the 2- and 5-positions (Scheme 1), providing a large number of observable transitions for  $[2^{-2}H]$ -,  $[5^{-2}H]$ -, and  $[2,5^{-2}H]$ -thiazole. The spectroscopic constants of  $[2^{-2}H]$ -thiazole and  $[2,5^{-2}H]$ -thiazole have been reported, recently, and

are included in the dataset for the current study.<sup>29</sup> The dataset of  $[2,5-^2H]$ -thiazole contains over 4300 transitions and resulted in the determination of a full set of quartic and sextic centrifugal distortion constants. Due to the lower abundance of  $[2,5-^2H]$ -thiazole in the sample, fewer heavy-atom isotopologues were observed, and a smaller number of transitions were measured for the isotopologues that were observed. Despite this limitation, spectroscopic constants were determined for  $[2,5-^2H,\ ^{34}S]$ -,  $[2,5-^2H,\ 2-^{13}C]$ -,  $[2,5-^2H,\ 4-^{13}C]$ -, and  $[2,5-^2H,\ 5-^{13}C]$ -thiazole. A 272–277 GHz

TABLE II. Spectroscopic constants of thiazole isotopologues (S-reduced Hamiltonian, I<sup>r</sup> representation).<sup>a</sup>

	$[^{34}S]$	$[2^{-13}C]$	$[4-^{13}C]$	$[5-^{13}C]$	$[^{33}S]$	$[^{15}N]$
$A_0^{(S)}$ (MHz)	8 529.150 84(12)	8 335.761 73(53)	8 461.036 76(37)	8 317.902 02(44)	8 529.230(25)	8 471.085(95)
$B_0^{(S)}$ (MHz)	5 353.296 193(76)	5 504.961 13(21)	5 412.744 11(20)	5 506.021 25(21)	5 427.491(11)	5 401.334(41)
$C_0^{(S)}$ (MHz)	3 287.365 421(81)	3 313.795 72(15)	3 299.384 84(13)	3 311.351 32(12)	3 315.217 42(31)	3 296.665 78 (48)
$D_J$ (kHz)	0.744 675(53)	0.76671(10)	0.741 83(12)	0.765 18(17)	0.75963(32)	0.74291(75)
$D_{JK}$ (kHz)	0.61462(14)	0.61375(60)	0.64800(58)	0.609 67 (91)	[0.596 247]	[0.626 671]
$D_K$ (kHz)	1.880 96(22)	1.73689(80)	1.799 25(66)	1.742 23(89)	[1.88017]	[1.79954]
$d_1$ (kHz)	-0.317225(15)	-0.335557(34)	-0.319650(67)	-0.335356(84)	-0.32559(24)	-0.31897(58)
$d_2$ (kHz)	-0.065 959 5(61)	-0.071 959(11)	-0.068112(10)	-0.071 971(12)	-0.067724(86)	-0.06732(23)
$H_J$ (Hz)	0.000273(12)	0.000259(24)	0.000260(39)	0.000 299(69)	0.000243(29)	0.000 383(75)
$H_{JK}$ (Hz)	-0.002228(61)	-0.00224(24)	-0.00238(27)	-0.00282(34)	[-0.002168]	[-0.00191]
$H_{KJ}$ (Hz)	0.00261(12)	[0.002924]	0.003 35(55)	[0.0027823]	[0.0026976]	[0.0023576]
$H_K$ (Hz)	0.001 09(15)	[0.000765]	[0.000 842]	[0.000 813 3]	[0.0009399]	[0.000 936 3]
$h_1$ (Hz)	0.000 138 4(31)	[0.000 131 9]	0.000 129(20)	0.000 172(35)	[0.0001294]	[0.0001225]
$h_2$ (Hz)	0.000 032 4(20)	[0.000 030 5]	[0.0000326]	[0.000 031 9]	[0.000 032 3]	[0.000 035 6]
$h_3$ (Hz)	0.000 020 36(37)	[0.0000226]	0.000 019 9(28)	[0.0000226]	[0.0000209]	[0.0000205]
$N_{ m lines}^{ m \ \ \ \ \ \ \ \ \ \ \ \ \ \ \ \ \ \ \$	1 741	557	645	547	190 <sup>c</sup>	103
$\sigma_{\rm fit}$ (MHz)	0.031	0.037	0.036	0.035	0.034	0.032
$\kappa^{\mathrm{d}}$	-0.212	-0.127	-0.181	-0.123	-0.189	-0.187
$\Delta_i (\mu \text{Å}^2)^e$	0.075402(4)	0.075 496(9)	0.075 202(7)	0.075 575(7)	0.07493(25)	0.07508(98)
	[2- <sup>2</sup> H] Ref. 29	[4- <sup>2</sup> H] Ref. 8	[5- <sup>2</sup> H]	$[2-^{2}H, {}^{34}S]$	[2,5- <sup>2</sup> H] Ref. 29	$[2-^{2}H, 2-^{13}C]$
$A_0^{(S)}$ (MHz)	7 867.574 136(46)	8 325.228(8)	7 855.905 82(39)	7 867.677 06(17)	7 278.097 529(42)	7 709.597 32(79)
$B_0^{(S)}$ (MHz)	5 505.480 154(41)	5 229.035(6)	5 498.490 87(13)	5 353.149 076(99)	5 498.436 111(39)	5 504.733 70(31)
$C_0^{(S)}$ (MHz)	3 237.418 276(49)	3 210.280(5)	3 233.020 39(12)	3 184.137 237 (93)	3 130.729 943(48)	3 210.080 13(23)
$D_I$ (kHz)	0.750 860(33)		0.743 404(77)	0.725 256(67)	0.728 060(30)	0.747 97(16)
$D_{JK}$ (kHz)	0.520010(25)		0.556 26(39)	0.501 64(23)	0.420 398(22)	0.49151(88)
$D_K$ (kHz)	1.384 483(33)		1.36000(50)	1.427 56(22)	1.042 394(26)	1.3330(10)
$d_1$ (kHz)	-0.338 667 7(52)		-0.335 780(25)	-0.322 476(25)	-0.3407523(44)	-0.340445(62)
$d_2$ (kHz)	-0.0739728(22)		-0.074 303 8(91)	-0.0690218(54)	-0.0764160(19)	-0.074727(20)
$H_J$ (Hz)	0.000 261 1(72)		0.000235(18)	0.000230(16)	0.000 246 3(63)	0.000 246(35)
$H_{JK}$ (Hz)	-0.0021510(48)		-0.00201(11)	-0.002011(98)	-0.001 761 8(43)	-0.00278(38)
$H_{KJ}$ (Hz)	0.002 743 1(95)		$[0.002\ 106\ 6]$	0.00201(18)	0.0022560(83)	[0.0029374]
$H_K$ (Hz)	0.000 430(11)		[0.0006446]	[0.000 467 8]	0.000 187 5(72)	[0.000 304]
$h_1$ (Hz)	0.000 129 18(99)		[0.000 125 2]	0.000 138 3(58)	0.000 121 77(71)	
$h_2$ (Hz)	0.000 035 74(67)		[0.000 037 1]	[0.000 026 4]	0.000 040 48(49)	
$h_3$ (Hz)	0.000 024 43(13)		0.0000256(15)	0.000 019 35(79)	0.000 025 14(10)	
$N_{\rm lines}^{}$	4 051	23	663	1 251	4 3 3 1	381
$\sigma_{\rm fit}$ (MHz)	0.025		0.035	0.032	0.026	0.040
κ <sup>d</sup>	-0.020	-0.211	-0.020	-0.074	0.142	0.020
$\Delta_i (\mu \text{Å}^2)^e$	0.074252(2)	0.07207(28)	0.074511(7)	0.075081(5)	0.073729(3)	0.075005(14)

TABLE II. (Continued.)

	$[2-^{2}H, 4-^{13}C]$	$[2-^{2}H, 5-^{13}C]$	$[2-^{2}H, ^{33}]$	S]	$[2-^{2}H, ^{15}N]$	$[2,5-^{2}H, ^{34}S]$	$[2,5-^{2}H,2-^{13}C]$
$A_0^{(S)} \text{ (MHz)}$ $B_0^{(S)} \text{ (MHz)}$ $C_0^{(S)} \text{ (MHz)}$	7 806.550 53(73) 5 411.488 92(24) 3 194.503 23(24)	7 679.630 26(60) 5 505.730 70(23) 3 205.209 77(20)	7 867.527(20 5 427.312(1 3 210.210 80	3)	7 821.202(87) 5 401.281(44) 3 193.389 82(36)	7 277.296 19(17) 5 347.685 929(85) 3 081.112 250(78)	7 137.702 07(69) 5 496.921 08(49) 3 103.967 03(11)
$D_{J}$ (kHz) $D_{JK}$ (kHz) $D_{K}$ (kHz) $d_{1}$ (kHz) $d_{2}$ (kHz)	0.720 53(15) 0.535 75(35) 1.367 7(11) -0.323 749(43) -0.071 006(14)	0.746 61(15) 0.481 89(66) 1.324 8(11) -0.340 330(51) -0.074 682(18)	0.740 42 [0.479 08 [1.433 75 -0.330 94 -0.070 55	[35] [33]	0.714 03(42) [0.500 11] 1.522(17) -0.317 33(23) [-0.068 030 1]	0.703 645(61) 0.405 73(31) 1.082 30(23) -0.325 048(28) -0.071 471 1(65)	0.726 40(26) 0.387 7(19) 1.005 0(20) -0.342 66(10) -0.076 908(49)
$H_{J}$ (Hz) $H_{JK}$ (Hz) $H_{KJ}$ (Hz) $H_{K}$ (Hz) $h_{1}$ (Hz) $h_{2}$ (Hz) $h_{3}$ (Hz)	0.000 231 (35) [-0.002 021 3] [0.002 624 4] [0.000 411] [0.000 125 3] [0.000 028] [0.000 021 9]	0.000 311(32) [-0.002 169 1] [0.002 860 1] [0.000 294 9] [0.000 129 7] [0.000 025 1] [0.000 024]	[0.000 23 [-0.002 10 [0.002 73 [0.000 42 [0.000 12 [0.000 02 [0.000 02	25] 33] 36] 7]	[0.000 213 2] [-0.001 874 9] [0.002 454 2] [0.000 422 5] [0.000 120 5] [0.000 030 4] [0.000 021 7]	0.000 257(20) -0.002 072(91) 0.001 86(23) [0.000 258 4] 0.000 159(10) [0.000 027] 0.000 021 2(11)	$ \begin{bmatrix} 0.000 \ 232 \ 3 \end{bmatrix} \\ \begin{bmatrix} -0.001 \ 837 \ 2 \end{bmatrix} \\ \begin{bmatrix} 0.002 \ 378 \ 2 \end{bmatrix} \\ \begin{bmatrix} 0.000 \ 142 \ 3 \end{bmatrix} \\ \begin{bmatrix} 0.000 \ 121 \ 6 \end{bmatrix} \\ \begin{bmatrix} 0.000 \ 025 \ 1 \end{bmatrix} \\ \begin{bmatrix} 0.000 \ 024 \ 6 \end{bmatrix} $
$N_{ m lines}^{ m b}$ $\sigma_{ m fit}  ({ m MHz})$ $\kappa^{ m d}$ $\Delta_i  (\mu { m \AA}^2)^{ m e}$	371 0.042 -0.039 0.074 868(14)	369 0.039 0.028 0.075 061(12)	147 0.038 -0.048 0.074 80	(31)	96 0.037 -0.046 0.0748(10)	1 348 0.029 0.080 0.074 632(5)	388 0.032 0.186 0.074 410(12)
	$[2,5-^{2}H,4-^{13}C]$	$[2,5-^2H,$	5- <sup>13</sup> C]	[2,	$5-^{2}H$ , $^{33}S$ ]	$[2,5-^{2}H,^{15}N]$	[2,4,5- <sup>2</sup> H]
$A_0^{(S)}$ (MHz) $B_0^{(S)}$ (MHz) $C_0^{(S)}$ (MHz)	7 224.702 94(51) 5 406.990 39(24) 3 091.125 251(98	) 5 498.578 4	13(32)	5 421.	719(14) 027 8(86) 404 52(16)	7 240.976(23) 5 390.551(14) 3 088.712 34(19)	7 124.736(23) 5 223.602(14) 3 012.615 79(26)
$D_J$ (kHz) $D_{JK}$ (kHz) $D_K$ (kHz) $d_1$ (kHz) $d_2$ (kHz)	0.701 489(98 0.417 84(81) 1.043 5(10) -0.327 050(54) -0.073 147(32)	) 0.381 5 1.015 3 4) -0.342 2	5(19) 3(16) 29(12)	[0. [1. -0.	719 45(24) 385 347] 088 56] 334 33(18) 073 562(66)	0.698 65(31) [0.425 291] [1.027 17] -0.325 00(23) -0.072 667(89)	0.633 55(32) [0.405 665] [1.040 61] -0.292 42(25) -0.065 25(10)
$H_J$ (Hz) $H_{JK}$ (Hz) $H_{KJ}$ (Hz) $H_K$ (Hz) $h_1$ (Hz) $h_2$ (Hz) $h_3$ (Hz)	[0.000 225 2] [-0.001 774 4] [0.002 314 4] [0.000 150 7] [0.000 120 8] [0.000 026 6] [0.000 022 9]	[-0.001 7 [0.002 2 [0.000 1 [0.000 1	7794] 2537] 1944] 1222]	[-0. [0. [0. [0.	000 221 5] 001 750 8] 002 234 7] 000 232 7] 000 120 4] 000 027 9] 000 023]	[0.000 190 2] [-0.001 423 5] [0.001 762 4] [0.000 348] [0.000 111 6] [0.000 034 2] [0.000 022 2]	[0.000 182 2] [-0.001 452 8] [0.001 794 1] [0.000 363 7] [0.000 100 6] [0.000 024 1] [0.000 018 5]
$N_{ m lines}^{ m b}$ $\sigma_{ m fit}$ (MHz) $\kappa^{ m d}$ $\Delta_i$ ( $\mu$ Å <sup>2</sup> ) <sup>e</sup>	405 0.032 0.121 0.074 302(8)	414 0.032 0.192 0.074 4	133(9)	0.	035 110 074 09(23)	0.039 0.109 0.074 18(33)	176 0.043 0.075 0.072 06(35)

 $<sup>\</sup>overline{\ ^{a}\text{Values in square brackets held fixed at the computed value [CCSD(T)/cc-pCVTZ] in least-squares fit.}$ 

<sup>&</sup>lt;sup>b</sup>Number of independent transitions.

 $<sup>^{\</sup>rm c}$  Includes six transitions using the hyperfine-free line center as reported in Ref. 14.

 $<sup>^{\</sup>mathrm{d}}\kappa=(2B-A-C)/(A-C).$ 

<sup>&</sup>lt;sup>e</sup>Inertial defect ( $\Delta_i = I_c - I_a - I_b$ ) calculated with PLANM.

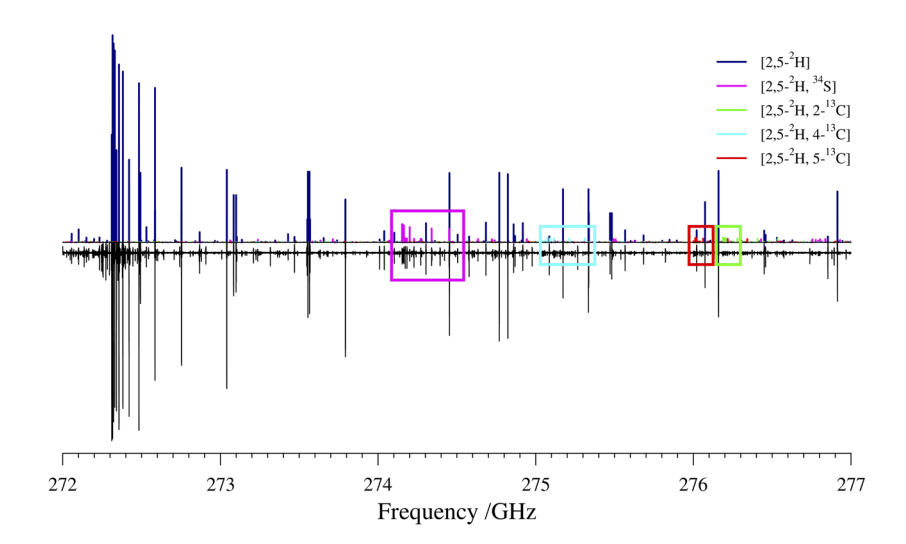


**FIG. 3.** Predicted (top) and experimental (bottom) rotational spectra of sample containing predominantly [2,5–2H]-thiazole from 272 to 277 GHz. The [2,5–2H, <sup>33</sup>S], [2,5–2H, <sup>15</sup>N], and [2,4,5–2H]-thiazole isotopologues were also observed in this spectrum, but their transitions are not highlighted due to being too low in intensity to resolve in this figure.

spectral segment from this sample showcases the relative intensities of the heavy-atom isotopologues in Fig. 3. For the  $^{13}$ C-isotopologues, only  $\sim$ 100 transitions for each could be assigned and least-squares fit. Depending on which transitions could be measured, *i.e.*, those whose frequencies were not substantially affected by incidental overlap with transitions from other isotopologues and vibrationally excited states, some of the quartic spectroscopic constants could be determined.

Spectroscopic constants from previous work are available for [4-2H]-thiazole.<sup>8,9</sup> The deuterium-enrichment methods [Scheme 1(a)-1(c)] presented in this work did not lead to significant H/D exchange at the 4-position. A trace amount of [2,4,5-2H]-thiazole was detected by GC-MS in a sample produced by base-catalyzed isotope exchange [1(b)], and this isotopologue was subsequently identified in the rotational spectrum. Semi-experimental equilibrium rotational constants were estimated for [2,4,5-2H]-thiazole using an initial  $r_e^{\text{SE}}$  structure derived from 19 other isotopologues. These equilibrium rotational constants, corrected by computational vibration-rotation interaction constants and electron-mass corrections and combined with computational sextic and quartic centrifugal distortion constants for [2,4,5-2H]-Thiazole, were used to locate the low-intensity transitions for this isotopologue.  $[2,4,5-^{2}H]$ -Thiazole was estimated as having <0.5% the intensity of  $[2,5^{-2}H]$ thiazole, the most abundant species in this sample. Searches for the  $[4-^2H]$ -,  $[2,4-^2H]$ -, and  $[4,5-^2H]$ -isotopologues were unsuccessful in each of our samples, even when using the  $r_e^{\rm SE}$  structure to predict their spectroscopic constants. This is unsurprising due to the aforementioned very slow incorporation of deuterium at the 4-position and the more rapid incorporation of deuterium at both 2- and 5-positions.

# Semi-experimental equilibrium structure ( $r_e^{SE}$ )

Using the spectroscopic data presented in this work, a semi-experimental equilibrium structure ( $r_e^{\rm SE}$ ) was determined using the *xrefit* module of CFOUR. To generate constants free of centrifugal distortion and the impact of the choice of an A- or S-reduced Hamiltonian, the rotational constants ( $B_0^x$ , where x = A, B, or C) determined in each least-squares fit were converted to determinable

constants ( $B_0''$ ) using Eqs. S1–S6 of the supplementary material. For each of the isotopologues presented in this work, differences in the determinable constants from the A and S reductions were quite small. The largest of these were observed for the <sup>33</sup>S isotopologue:

**TABLE III.** Inertial defects  $(\Delta_i)$  of thiazole isotopologues from various determinations of the moments of inertia.

Isotopologue	$\Delta_{i0} \; (\mu \mathring{\rm A}^2)$	$\Delta_{ie} (\mu \mathring{A}^2)^a$	$\Delta_{ie} (\mu \mathring{A}^2)^b$
$C_3H_3NS$	0.074 55	-0.009 30	0.001 24
[ <sup>34</sup> S]-	0.075 32	-0.00924	0.001 30
$[2-{}^{13}C]-$	0.07541	-0.00927	0.00128
$[4-^{13}_{12}C]$ -	0.075 11	-0.00931	0.00124
$[5-^{13}C]$ -	0.07549	-0.00928	0.001 26
[ <sup>33</sup> S]-	0.07480	-0.00940	0.001 14
[ <sup>15</sup> N]-	0.07507	-0.00927	0.001 27
$[2-^{2}H]$ -	0.074 16	-0.00951	0.001 03
$[4-^{2}H]$ -	0.072 18	-0.01012	0.00043
$[5-^{2}H]$ -	0.07442	-0.00961	0.00094
$[2-^{2}H, ^{34}S]-$	0.07499	-0.00945	0.001 09
$[2,5-^{2}H]$ -	0.073 64	-0.00983	0.00072
$[2-^{2}H, 2-^{13}C]$ -	0.07491	-0.00947	0.001 07
$[2-^{2}H, 4-^{13}C]$ -	0.07478	-0.00949	0.001 06
$[2-^{2}H, 5-^{13}C]$ -	0.07497	-0.00950	0.00104
$[2-^{2}H, ^{33}S]-$	0.07473	-0.00934	0.001 20
$[2-^{2}H, ^{15}N]-$	0.07470	-0.00940	0.001 10
$[2,5-^{2}H, ^{34}S]-$	0.07454	-0.00976	0.00079
$[2,5-^{2}H, 2-^{13}C]$ -	0.07432	-0.00977	0.00078
$[2,5-^{2}H,4-^{13}C]$ -	0.07421	-0.00978	0.00077
$[2,5^{-2}H,5^{-13}C]$ -	0.07434	-0.00979	0.00075
$[2,5-^{2}H, ^{33}S]-$	0.071 98	-0.00983	0.00072
$[2,5-^{2}H,^{15}N]$ -	0.07405	-0.00985	0.00070
$[2,4,5-^{2}H]$ -	0.07411	-0.00983	0.00072
Average (μ)	0.07445	-0.00956	0.00099
Std. dev. (s)	0.000 86	0.000 25	0.000 24

<sup>&</sup>lt;sup>a</sup>Vibration-rotation interaction corrections only.

<sup>&</sup>lt;sup>b</sup>Vibration-rotation interaction and electron-mass corrections.

20 Hz for  $A_0''$ , 11.5 Hz for  $B_0''$ , and 0.77 Hz for  $C_0''$ . Such close agreement between the spectroscopic constants obtained by the least-squares fits provides confidence that the  $A_0''$ ,  $B_0''$ , and  $C_0''$ values are reliable. These determinable constants were averaged and used in the  $r_e^{\rm SE}$  structure determination after correcting for the vibration-rotation interactions and electron-mass distributions. The averaged determinable constants are provided in Table SII. The quality of the spectroscopic constants, vibration-rotation interaction constants, and electron-mass corrections is apparent from the inertial defects  $(\Delta_i)$  displayed in Table III. For a planar molecule, free of vibration-rotation interaction, the inertial defect should be zero. Both the vibration-rotation interaction constants and electron-mass corrections reduce the absolute value of the inertial defect by about an order of magnitude, resulting in a decrease in the total average correction of the inertial defect from 0.07445 to  $0.000\,99\,\mu\text{Å}^2$ . This correction is similar to that seen in other planar, heteroaromatic compounds with rotational constants treated with CCSD(T) corrections. 20,25,31 Typically, the vibration–rotation interaction correction over-corrects the initially slightly positive inertial defects ( $\Delta_{i0}$ ) and results in negative values. These values, in turn, are counter-corrected by the electron-mass correction to slightly positive values. The systematic nature of the isotopologue inertial defect corrections indicates an unknown systematic issue, which is the result of an imperfect or incomplete correction of the experimental rotational constants. Nevertheless, the fully corrected average residual inertial defect ( $\Delta_{ie}$ ) of 0.00 099 (24)  $\mu \mathring{A}^2$  is sufficiently small to produce a very precise  $r_e^{SE}$  structure. Comparing this  $\Delta_{ie}$  value to the corresponding result from thiophene, [0.00 117 (16)  $\mu \mathring{A}^2$ ], creveals that the two results are not different within the statistical uncertainty of the former. This agreement is further evidence that there is a highly systematic, untreated error despite the high-level corrections in this work.

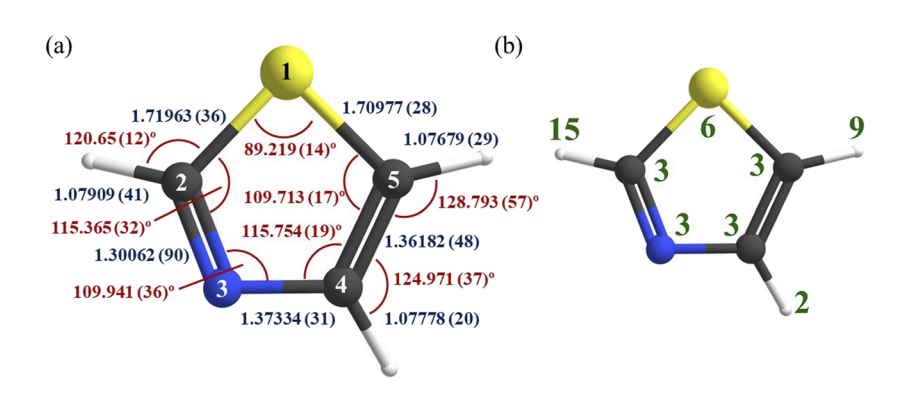
The corrected  $B_e^x$  constants for each isotopologue were converted to their corresponding moments of inertia  $(I_e^x)$  and used in *xrefit* to produce the  $r_e^{\text{SE}}$  structure presented in Table IV and Fig. 4(a). The  $C_s$  structure of thiazole has 13 independent structural parameters (seven bond distances and six bond angles), which are redundantly determined from 72 moments of inertia, of which 48 are independent. Each of the atoms of thiazole is isotopically substituted at least twice in the  $r_e^{\rm SE}$  structure dataset, with the N(3) and H(C4) being the least substituted. Due to the ease of substituting H(C2), this position bears deuterium in about half of the isotopologues and enables multiple isotopic substitutions of each heavy atom. The resulting  $r_e^{\rm SE}$  bond distances have  $2\sigma$  statistical uncertainties of  $\leq 0.0009$  Å. The bond angles have  $2\sigma$  statistical uncertainties of <0.04°, with the exception of two bond angles involving H-atoms at C5 and C2 that exhibit  $2\sigma$  statistical uncertainties of 0.057° and 0.12°, respectively. As shown in Fig. 4(b), the most poorly determined angle is  $\theta_{S-C2-H}$ , which contains atoms that are isotopically substituted 6, 3, and 15 times, respectively.

TABLE IV. Structural parameters of thiazole.

	r <sub>e</sub> <sup>SE</sup> (Ref. 18) B2PLYP/ cc-pVTZ <sup>a</sup>	r <sub>e</sub> <sup>SE</sup> CCSD(T)/ cc-pCVTZ	$r_e^{ m SE}$ CCSD(T)/ cc-pCVTZ	CCSD(T) BTE	CCSD(T)/ cc-pCV5Z	CCSD(T)/ cc-pCVQZ	CCSD(T)/ cc-pCVTZ
R <sub>C4-C5</sub> (Å)	1.3645 (18)	1.361 77 (50)	1.361 82 (48)	1.3632	1.3630	1.3634	1.3653
$R_{\rm S1-C5}$ (Å)	1.7089 (10)	1.709 80 (28)	1.709 77 (28)	1.7094	1.7087	1.7106	1.7174
$R_{\text{C5-H}}$ (Å)	1.0753 (12)	1.076 77 (31)	1.07679(29)	1.0757	1.0756	1.0757	1.0765
R <sub>С4-Н</sub> (Å)	1.0774(8)	1.077 78 (19)	1.07778(20)	1.0780	1.0779	1.0781	1.0790
$R_{ m N3-C4}$ (Å)	$1.3720(32)^{b}$	1.373 40 (32)	1.373 34 (31)	1.3733	1.3726	1.3735	1.3773
$R_{S1-C2}$ (Å)	1.7213 (14)	1.719 67 (37)	1.719 63 (36)	1.7197	1.7181	1.7201	1.7272
$R_{\mathrm{C2-H}}$ (Å)	1.0801 (23)	1.079 19 (41)	1.079 09 (41)	1.0783	1.0782	1.0783	1.0792
$R_{\rm C2-N3}$ (Å)	1.2986 (20)	$1.3005(10)^{b}$	$1.30062(90)^{b}$	$1.3018^{b}$	$1.3014^{b}$	1.3019 <sup>b</sup>	1.3041 <sup>b</sup>
$R_{\rm S1-N3}  (\text{Å})^{\rm b}$	2.5616 (22)	2.562 50 (80)	2.562 52 (73)	2.5634	2.5616	2.5646	2.5758
$R_{\rm S1-C4}  (\rm \mathring{A})^{\rm b}$	2.5202 (19)	2.519 68 (52)	2.519 63 (46)	2.5203	2.5188	2.5209	2.5291
$R_{\text{C2-C5}} (\text{Å})^{\text{b}}$	2.4094 (16)	2.408 32 (46)	2.408 70 (40)	2.4089	2.4082	2.4094	2.4139
$R_{\mathrm{H(C2)-H(C4)}} (\text{Å})^{\mathrm{b}}$	4.1699 (57)	4.168 5 (12)	4.169 5 (11)	4.1665	4.1658	4.1666	4.1707
$\theta_{\text{S1-C5-C4}}$ (deg)	109.66(6)	109.716 (16)	109.713 (17)	109.705	109.657	109.670	109.729
$\theta_{\text{C4-C5-H}}$ (deg)	128.51 (22)	128.778 (58)	128.793 (57)	128.535	128.527	128.519	128.456
$\theta_{\text{C5-C4-H}}$ (deg)	125.04 (12)	124.968 (37)	124.971 (37)	125.022	124.955	124.919	124.854
$\theta_{\text{N3-C4-C5}}$ (deg)	115.70 (15)	115.751 (19)	115.754 (19)	115.750	115.760	115.807	115.957
$\theta_{\text{C2-S1-C5}}$ (deg)	89.24 (5)	89.214 (14)	89.219 (14)	89.254	89.298	89.225	88.980
$\theta_{\text{S1-C2-H}}$ (deg)	120.27 (63)	120.63 (11)	120.65 (12)	120.898	120.926	120.887	120.753
$\theta_{\rm S1-C2-N3} (\rm deg)^b$	115.33 (06)	115.390 (36)	115.365 (32)	115.378	115.372	115.434	115.661
$\theta_{\text{C2-N3-C4}} (\text{deg})^{\text{b}}$	110.07 (14)	109.929 (40)	109.941 (36)	109.913	109.913	109.864	109.674
$\theta_{\text{N3-C4-H}} (\text{deg})^{\text{b}}$	119.26 (19)	119.281 (40)	119.263 (38)	119.228	119.285	119.274	119.189
$N_{ m isotopologues}$	9	21	24				

<sup>&</sup>lt;sup>a</sup>Statistical uncertainties as listed in Ref 18.

<sup>&</sup>lt;sup>b</sup>Value and uncertainty determined from the  $r_e^{\text{SE}}$  structure using the alternate Z-matrix described in the supplementary material.



**FIG. 4.** (a) Semi-experimental equilibrium structure  $(r_e^{\rm SE})$  of thiazole with  $2\sigma$  statistical uncertainties from least-squares fitting the isotopologue moments of inertia. The values of  $R_{\rm C2-N3}$ ,  $\theta_{\rm C2-N3-C4}$ , and  $\theta_{\rm S1-C2-N3}$  were determined from the  $r_e^{\rm SE}$  structure using the alternate Z-matrix described in the supplementary material. (b) Number of isotopologues with a substitution relative to the main isotopologue ( $C_3H_3NS$ ) at the labeled atom.

Table IV presents the previous B2PLYP  $r_e^{\text{SE}}$  structure, the current CCSD(T)  $r_e^{\text{SE}}$  structure using only 21 isotopologues (excluding the [2,5–<sup>2</sup>H, <sup>15</sup>N]-, [<sup>33</sup>S]-, and [2,5–<sup>2</sup>H, <sup>33</sup>S]-isotopologues, *vide infra*), the current CCSD(T)  $r_e^{\text{SE}}$  structure using all 24 isotopologues, and several CCSD(T) theoretical structures.

## **DISCUSSION**

# Influence of multiple isotopic substitutions on structure determination ( $r_e^{SE}$ )

Many structure determinations via rotational spectroscopy have relied upon single isotopic substitution at each unique atom to provide the minimum structural information to define a molecular structure. This approach satisfies the requirements for using Kraitchman's equations<sup>40</sup> to determine the principal axis Cartesian coordinates of each atom by comparing the moments of inertia of a reference molecule to those of an isotopologue. This procedure has not changed significantly, even with the development of modern least-squares fitting methods to determine  $r_0$  or  $r_e^{SE}$  structures and their ability to use all available isotopologue rotational data, because of the difficulty of obtaining samples of multiply

substituted isotopologues. The obvious advantage of utilizing multiple isotopic substitutions of many or all of the atoms in a molecule is that the redundant information should refine each atom's position in the molecule, leading to a better statistical determination of the  $r_e^{\rm SE}$  parameters, <sup>20,26</sup> as we recently demonstrated for pyridazine  $(o-C_4H_4N_2)$ , <sup>20</sup> hydrazoic acid  $(HN_3)$ , <sup>41</sup> pyrimidine  $(m-C_4H_4N_2)$ , <sup>25</sup> and thiophene  $(C_4H_4S)$ . <sup>31</sup> As shown in Fig. 5 for thiazole, the addition of isotopologues beyond those that singly substitute each atom causes a dramatic decrease in the statistical uncertainties of the structural parameters. The plot in Fig. 5 shows the square root of the sum of the squares for the relative statistical uncertainties of each parameter type [Eq. (1), using  $2\sigma$  uncertainties] as a function of the number of isotopologues used by xrefit to determine  $r_e^{\rm SE}$ ,

$$\delta r_e^{\rm SE} = \sqrt{\sum \left(\frac{\text{uncertainty of parameter}}{\text{value of parameter}}\right)^2}.$$
 (1)

The initial set of nine isotopologues of thiazole was used to generate an  $r_e^{\rm SE}$  structure that is based upon the traditional method involving single isotopic substitution, including [ $^{34}$ S]- and excluding [ $^{33}$ S]-thiazole. Additional isotopologues are added to the structure

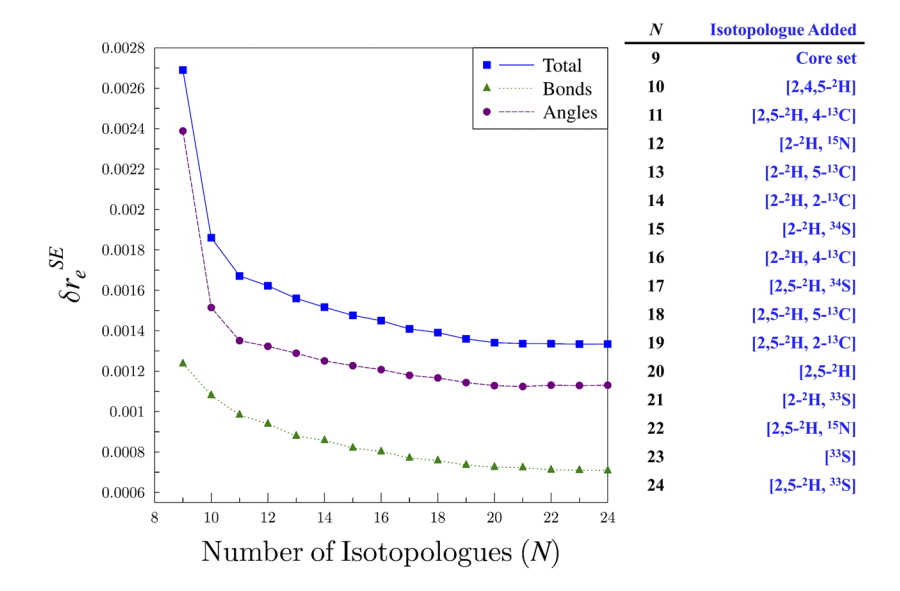


**FIG. 5.** Plot of  $\delta r_e^{\rm SE}$  as a function of the number of isotopologues (*N*) incorporated into the structure determination dataset. The total relative statistical uncertainty ( $\delta r_e^{\rm SE}$ , blue squares), the relative statistical uncertainty in the bond distances (green triangles), and the relative statistical uncertainty in the angles (purple circles) are presented.

determination, one at a time, with that which affords the greatest improvement in  $\delta r_e^{\rm SE}$  always added next. Although this iterative approach does not change the fact that the molecular structure is a state function of the rotational constants supplied to the fitting program, it reveals insight into the contributions of the additional isotopologues in refining the structure. The xrefiteration plot demonstrates the impact of having just a few additional isotopologues beyond the minimum necessary to obtain a complete structure (Fig. 5). An increase from nine to fourteen isotopologues reduces the  $\delta r_e^{\rm SE}$  by about 50%. Including additional isotopologues in the structure determination continues to reduce the  $\delta r_e^{\tilde{\text{SE}}}$ , except for the final three isotopologues ([2,5– $^2$ H,  $^{15}$ N], [ $^{33}$ S]-, and [2– $^2$ H,  $^{33}$ S]-thiazole), which slightly increase the angles'  $\delta r_e$   $^{SE}$ , resulting in a very slight increase in the  $\delta r_e^{\rm SE}$  upon addition of the 24th isotopologue. For this reason, we calculated the  $r_e^{\rm SE}$  structure with these three isotopologues excluded (Table IV). It is clear that the structure is largely unchanged by the inclusion or exclusion of these isotopologues. Each of these three isotopologues includes a relatively low number of transitions in their least-squares fits. Other low-transition isotopologues, however, do not have the same impact, e.g., [2-2H, 15N]-thiazole. This contrast in the behavior of different low-transition isotopologues makes it ambiguous as to whether additional transition measurements would improve the structure determination. The over-determination (or redundant determination) of the  $r_e^{SE}$  structure clearly has a useful impact on lowering the statistical uncertainty of each parameter. As was shown for thiophene,<sup>31</sup> however, there is a limit to the improvement seen in the statistical uncertainty by the addition of more isotopologues, and the cause of the increase in  $\delta r_e^{\rm SE}$  for the last few isotopologues is

In addition to lowering the statistical uncertainty of each parameter, the inclusion of many isotopologues beyond the minimum set of single-substitution isotopologues (core set) is likely to increase the accuracy of each parameter, as revealed by comparisons to high quality theoretical predictions. Initially, the inclusion of additional isotopologues can have a substantial impact relative to the parameter value determined by the core set. With the addition of many more isotopologues, however, the impact of each additional isotopologue should be reduced, and the parameter value should begin to converge. As shown in Fig. 6, the value of  $\theta_{\text{C4-C5-H}}$ does not appear to converge until 16 isotopologues are included in the  $r_e^{SE}$ . As additional isotopologues are added, the value does not change by more than 0.0007°. For several of the distance parameters, it appears that the inclusion of 14 or more isotopologues is required to converge the value within 0.0001 Å of the final value. Likewise, the angle parameters involving H atoms appear to require at least 16 isotopologues to be converged to within 0.03° of their final values. Importantly, the parameters that show the most variability  $(R_{\rm C2-H}, R_{\rm C2-S}, \text{ and } \theta_{\rm S-C2-H})$  upon initial inclusion of additional isotopologues involve C2, which is located very close to the b-axis. The difficulty in determining the atom positions of C2 and C5 for thiazole was well established previously,8 and it is consistent with the similar problem that arose in a recent  $r_e^{\text{SE}}$  determination of thiophene.<sup>31</sup> These challenges in determining the atom positions of C2 and C5 exist despite the <sup>13</sup>C-isotopic substitution of these atoms in three different isotopologues each, providing further evidence that the structural uncertainty has a systematic cause (vide infra). Despite these remaining structural ambiguities, all other parameters appear to be sufficiently stable upon addition of the final isotopologues that we expect the determined parameters to be reliable, and that they can be compared to high-level computational structures with some confidence. Finally, it is evident that although some of the parameter values determined using only the core set fall within the uncertainty of the final value, other values do change notably upon further addition of isotopologues to the least-squares fit, and many of the parameters demonstrate the expected decrease in uncertainty upon inclusion of additional isotopologues.

# A best theoretical estimate for the equilibrium structure of thiazole

We recently showed that excellent agreement can be achieved between semi-experimental equilibrium geometries obtained from the method described above and high-level theoretical structures.<sup>25,31</sup> For pyrimidine,<sup>25</sup> the agreement between the "best theoretical estimate" (BTE) structure and the  $r_e^{\rm SE}$  bond lengths was within roughly 0.0001 Å, which is remarkable and, in fact, comparable to a nuclear diameter. To achieve this agreement, theoretical approaches beyond a CCSD(T)/cc-pCV5Z calculation were required. As in the case of pyrimidine, a CCSD(T)/cc-pCV5Z calculation, alone, is insufficient to replicate the  $r_e^{SE}$  structure obtained in this work. As shown in Fig. 7, several of the structural parameters calculated at that level of theory fall outside the  $2\sigma$ statistical uncertainties of the  $r_e^{\rm SE}$  parameters. While an all-electron CCSD(T)/cc-pCV5Z calculation is considered a very high level of theory, especially for a molecule containing a third-row element, this method is limited in its treatment of electron correlation and its basis set. The theoretical structure can be further corrected for relativistic effects and the diagonal Born-Oppenheimer correction. To provide the best comparison to the semiexperimental equilibrium structure, the following four computational corrections to the CCSD(T)/cc-pCV5Z structure have been implemented to address remaining errors in the computational structure:

- 1. Residual basis set effects beyond cc-pCV5Z.
- Residual electron correlation effects beyond the CCSD(T) treatment.
- 3. Effects of scalar (mass-velocity and Darwin) relativistic effects.
- 4. Diagonal Born-Oppenheimer correction (DBOC).

These four corrections are obtained by a process similar to that implemented for pyrimidine,  $^{25}$  using Eqs. (2)–(8), and they are summarized in Table V.

 To estimate the correction needed to approach the infinite basis set limit, equilibrium structural parameters obtained with the cc-pCVXZ (X = D, T, Q, and 5) basis sets were extrapolated using the empirical exponential<sup>42</sup> expression in the following equation:

$$R(x) = R(\infty) + Ae^{-Bx}.$$
 (2)

R(x) are the values of the parameters obtained using the various basis sets (x = 2, 3, 4, and 5), and  $R(\infty)$  is the desired basis set limit estimate. Using three basis sets (x = 3, 4, and 5), the system of equations using Eq. (2) can be solved, yielding the

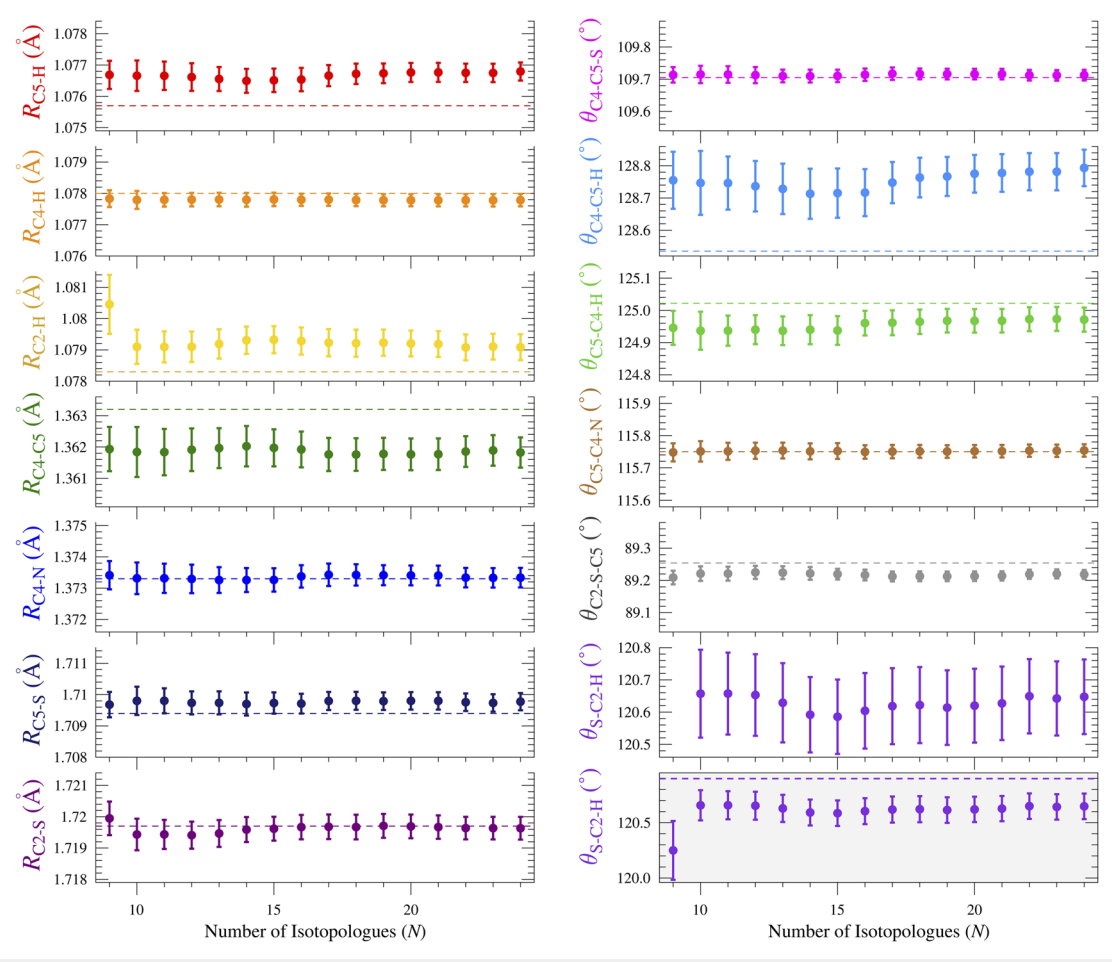


**FIG. 6.** Plots of the structural parameters as a function of the number of isotopologues (N) and their  $2\sigma$  uncertainties with consistent scales for each distance and for each angle. The dashed line in each plot is the BTE value calculated for that parameter. A plot of  $\theta_{S-C2-H}$  is additionally provided on a separate y-axis scale (gray background) that enables visualization of all data points and corresponding error bars. The isotopologue ordering along the x-axis is the same as that in the plot in Fig. 5.

following equation:

$$R(\infty) = -\frac{R(4)^2 - R(3)R(5)}{R(3) + R(5) - 2R(4)}.$$
 (3)

The correction to the structure due to a finite basis set is then estimated by the following equation:

$$\Delta R(\text{basis}) = R(\infty) - R(\text{CCSD}(T)/\text{cc-pCVTZ}).$$
 (4)

 Residual correlation effects are assessed by doing geometry optimizations at the CCSDT(Q) level<sup>43</sup> and then estimating the correlation correction in the following equation:

$$\Delta R(\text{cor}) = R(\text{CCSDT}(Q)) - R(\text{CCSD}(T)). \tag{5}$$

As calculations at the CCSDT(Q) level of theory are quite expensive, these two calculations are obtained with the cc-pVDZ basis, in the frozen-core approximation.

3. The relativistic corrections are obtained by subtraction of the equilibrium parameters obtained with a standard nonrelativistic calculation from those obtained with the X2C-1e variant of coupled-cluster theory, 44-46 as shown in the following equation:

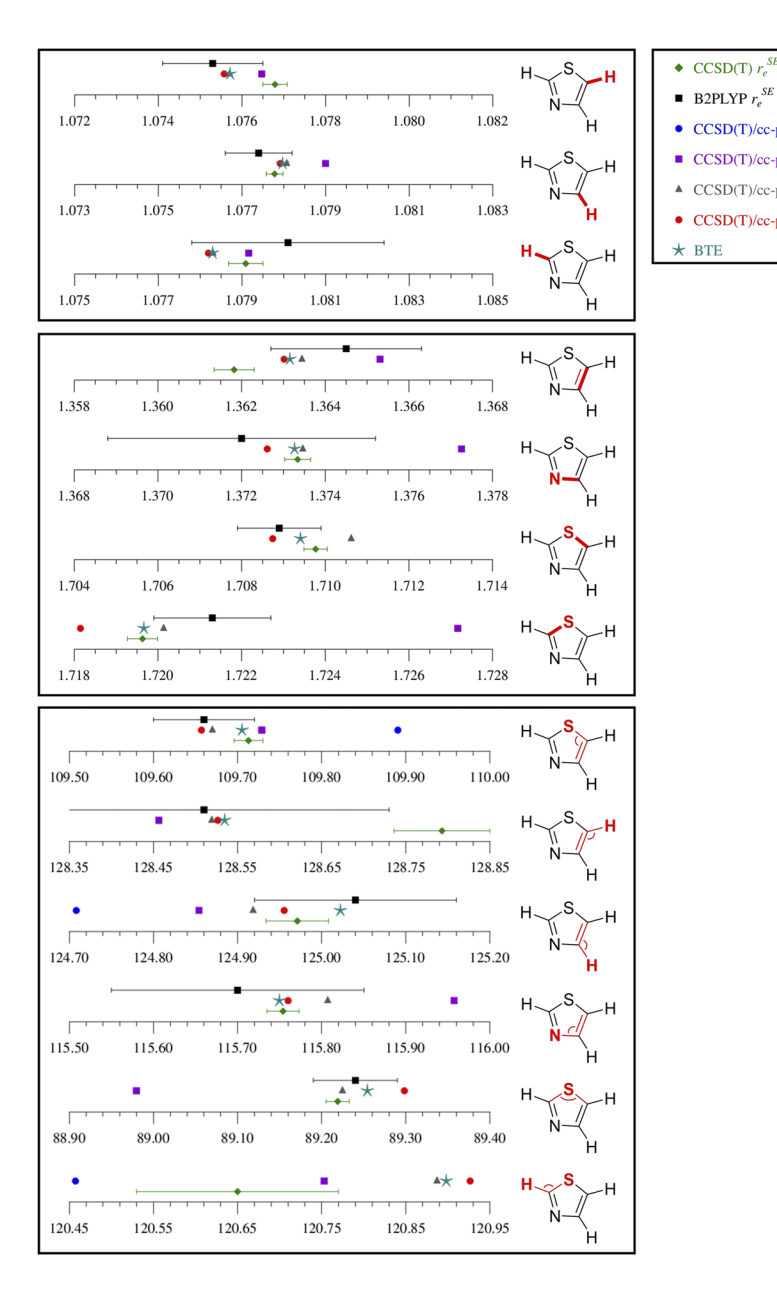
$$\Delta R(\text{rel}) = R(\text{CCSD}(T)/\text{cc-pCVTZ})_{\text{SFX2C-1e}} - R(\text{CCSD}(T)/\text{cc-pCVTZ})_{NR}.$$
 (6)

4. The diagonal Born–Oppenheimer correction (DBOC)<sup>47</sup> is obtained from the following equation:

$$\Delta R(DBOC) = R(SCF/cc-pCVTZ)_{DBOC} - R(SCF/cc-pCVTZ)_{NR}.$$
 (7)

Here, the first value is obtained by minimizing the DBOC-corrected SCF energy with respect to nuclear positions, and the latter is again the traditional calculation.

CCSD(T)/cc-pCVDZ CCSD(T)/cc-pCVTZ



CCSD(T)/cc-pCVOZ CCSD(T)/cc-pCV5Z

FIG. 7. Graphical comparison of the thiazole structural parameters with bond distances in angstroms (Å) and angles in degrees (°). The bond distances are set to the same scale, and the bond angles are set to the same scale. Uncertainties shown for current CCSD(T)  $r_e^{SE}$  are  $2\sigma$ , while those for the B2PLYP  $r_e^{\rm SE}$  are as reported in Ref. 18. Where symbols of predicted values do not appear, they are sufficiently far from the CCSD(T)  $r_e^{SE}$  as to not fit within the respective displayed ranges.

The best equilibrium structural parameters (BTE) are obtained by applying the sums of the corrections,  $\Delta R(\text{best})$ , from Eq. (8),

$$\Delta R(\text{best}) = \Delta R(\text{basis}) + \Delta R(\text{cor}) + \Delta R(\text{rel}) + \Delta R(\text{DBOC})$$
 (8)

to the CCSD(T)/cc-pCV5Z structural parameters (Table V). The resultant structural parameters are depicted in Fig. 7. We refer to them as the "best theoretical estimate" parameters.

As shown in Fig. 7, the agreement between the  $r_e^{\text{SE}}$  and the BTE  $r_e$  structural parameters is not as satisfactory as that in our previous

works. 25,31 For only four of the 13 parameters does the  $r_e$  parameter fall within the very narrow  $2\sigma$  value of the  $r_e^{\rm SE}$  parameter. For three more, the  $r_e$  parameters fall just outside of the  $2\sigma$  statistical uncertainty of the  $r_e^{\text{SE}}$  parameter. For six of the parameters, the  $r_e$ and  $r_e^{\text{SE}}$  values do not show close agreement at the statistical level of precision. The largest percentage difference (0.21%) occurs for the parameter that also has the largest uncertainty in the  $r_e^{\rm SE}$ ,  $\theta_{\rm S1-C2-H}$ , where there is a 0.25° discrepancy between the computed and semiexperimental values. This result is similar to that observed with thiophene, <sup>31</sup> where  $\theta_{S1-C2-H}$  is the parameter with the largest discrepancy (0.176°). The second-largest discrepancy (0.26° or 0.20%) between the  $r_e$  and  $r_e^{\rm SE}$  values of thiazole occurs in the  $\theta_{\rm C4-C5-H}$  angle.

TABLE V. Corrections used in determining the best theoretical estimate of equilibrium structural parameters of thiazole.

	Basis set correction [Eq. (4)]	Correlation correction [Eq. (5)]	Relativistic correction [Eq. (6)]	DBOC correction [Eq. (7)]	Sum of corrections [Eq. (8)]	CCSD(T)/ cc-pCV5Z	CCSD(T) BTE
R <sub>C4-C5</sub> (Å)	-0.000 126 3	0.000 637 1	-0.000 376 9	0.000 005 4	0.000 139 3	1.3630	1.3632
$R_{\rm S1-C5}$ (Å)	-0.0007246	0.001 267 8	0.000 109 1	0.0000106	0.0006627	1.7087	1.7094
$R_{\mathrm{C5-H}}$ (Å)	-0.0000259	0.0001264	-0.0000954	0.0001357	0.000 140 9	1.0756	1.0757
R <sub>C4-H</sub> (Å)	-0.0000311	0.0000759	-0.0001195	0.0001334	0.0000587	1.0779	1.0780
$R_{\mathrm{N3-C4}}$ (Å)	-0.0002461	0.0007920	0.0000531	0.0000547	0.000 653 7	1.3726	1.3733
$R_{\rm S1-C2}$ (Å)	-0.0007835	0.0022047	0.0000909	0.000 003 6	0.001 515 8	1.7181	1.7197
$R_{\mathrm{C2-H}}$ (Å)	-0.0000163	0.0000590	-0.0000863	0.0001437	$0.000\ 100\ 0$	1.0782	1.0783
$\theta_{\text{S1-C5-C4}}$ (deg)	-0.0036605	0.035 915 9	0.0163784	-0.0004404	0.048 193 4	109.657	109.705
$\theta_{\text{C4-C5-H}}$ (deg)	0.0009190	-0.0129315	0.0209180	-0.0008015	0.0081040	128.527	128.535
$\theta_{\text{C5-C4-H}}$ (deg)	0.049 324 5	0.0064928	0.0096454	0.001 294 9	0.066 757 6	124.955	125.022
$\theta_{\text{N3-C4-C5}}$ (deg)	-0.0214873	0.005 326 5	0.007 360 1	-0.0015715	-0.0103722	115.760	115.750
$\theta_{\text{C2-S1-C5}}$ (deg)	0.031 614 3	-0.0470563	-0.0313521	0.002 796 3	-0.0439977	89.298	89.254
$\theta_{\text{S1-C2-H}}$ (deg)	0.016 307 4	-0.015 382 1	-0.032 999 5	0.003 708 9	-0.028 365 3	120.926	120.898

Noteworthy is that this angle also involves an atom (C5) lying close to the b-axis. The larger discrepancy here may be partially explained by the larger number of structural parameters (13 for thiazole compared to eight for thiophene) determined from the same number of independent moments of inertia.

It is apparent that even with substantial improvements in the structure determination methodology, the problem first identified by Nygaard et al.8—the proximity of some atoms to a principal axis—remains an intrinsic problem that has not been remedied. Our previous analysis of thiophene also demonstrated that the proximity of the C2 and C2' atoms to the b-axis made precise determination of their a-coordinates particularly challenging. Given the very close structural similarity between thiazole and thiophene, it is not surprising that the same issues arise in the  $r_e^{SE}$  determination of both. The large mass of the sulfur atom causes the adjacent C2 and C5 atoms to be located very close to the b-axis and prevents substantial rotation of the principal axes upon isotopic substitution. Thus, it is reasonable that the two bond distances not involving C2 or C5 ( $R_{N-C4}$  and  $R_{C4-H}$ ) are among the parameters showing the best agreement between the BTE  $r_e$  and the  $r_e$  SE. Similarly, the two non-H-containing angles that show the best agreement between the BTE  $r_e$  and  $r_e^{SE}$  are those involving C4, C5, and one of the heteroatoms, whereas the largest discrepancy of the non-H-containing angles occurs for that involving both C2 and C5 ( $\theta_{C2-S1-C5}$ ).

To explore the origin of the discrepancies in the C2 and C5 locations, several additional structural parameters were determined from the  $r_e^{\rm SE}$  and  $r_e$  structures and are presented in Table IV. Although not directly optimized in the least-squares fitting of the structure, these additional parameters are in generally the same agreement as the least-squares fitted parameters. The BTE values of the additional angles ( $\theta_{\rm S1-C2-N3}$ ,  $\theta_{\rm C2-N3-C4}$ , and  $\theta_{\rm N3-C4-H}$ ) fall within their statistical uncertainties. For only one of the five additional distances,  $R_{\rm C2-C5}$ , do the values of the BTE parameters fall within the statistical uncertainties of their  $r_e^{\rm SE}$  values. Interestingly, this parameter involves both troublesome atoms C2 and C5. The close agreement between these two values may be due to the fact

that most of the error in the determined atom positions is in their a-axis coordinates, not their b-axis coordinates, and that  $R_{\rm C2-C5}$  lies nearly parallel to the b-axis. All of the observed behavior provides strong evidence that the close proximity of C2 and C5 to the b-axis, creating very small a-axis coordinates, is the primary source of the poorly determined  $r_e^{\rm SE}$  structural parameters.

## CONCLUSION

A precise semi-experimental structure ( $r_e^{SE}$ ) has been determined for the heterocyclic molecule thiazole (c<sup>-</sup>C<sub>3</sub>H<sub>3</sub>NS). The statistical uncertainty of each structural parameter is greatly reduced, and the accuracy of each parameter is improved for the current CCSD(T)-corrected  $r_e^{SE}$  compared to the previous DFT-corrected  $r_e^{\rm SE}$ . These improvements are attributable to three factors: (1) improved values of the experimental rotational constants of nine isotopologues used in the previous structure determination, (2) inclusion of rotational constants from 15 additional isotopologues, and (3) superior CCSD(T) corrections for vibration-rotation coupling and the effects of electron mass. The constants used in both the original substitution-structure determination  $(r_s)$  and subsequent DFT-corrected  $r_e^{SE}$  were produced from data that included only rotational constants and did not account for the impact of centrifugal distortion.<sup>8,18</sup> While this impact is small in the frequency range of the original study (15-30 GHz),<sup>7,8</sup> it is significant in the frequency range of the present study. Not treating the centrifugal distortion does have a small impact on the rotational constants, which becomes important for an  $r_e^{SE}$  structure at this level of precision. As clearly demonstrated in Figs. 5 and 6, the incorporation of data from additional isotopologues has a profound impact on the precision and the accuracy of  $r_e^{SE}$ . Moments of inertia for the normal isotopologue and eight singly substituted isotopologues are sufficient to determine each atom location using a Kraitchman analysis8 and provide sufficient information for a redundant leastsquares fit structure (13 structural parameters and 18 independent moments of inertia).<sup>18</sup> It is clear from this work, however, that

moments of inertia of those nine isotopologues are insufficient to determine a highly precise equilibrium  $r_e^{\rm SE}$  that can be optimally compared to a CCSD(T) calculation with a large basis set. The precision and accuracy of molecular structure determinations are enhanced, substantially, by inclusion of moments of inertia from as many isotopologues as is practical for each molecule, which typically requires intentional synthesis or enrichment. Finally, as noted in previous works, <sup>25,31</sup> the current study establishes that the vibration–rotation interaction and electron–mass corrections from CCSD(T) calculations are, in practice, superior to those from DFT calculations.

Despite the quality of the structure determination in this work, fewer than half of the structural parameters show agreement between the  $r_e^{\rm SE}$  and the  $r_e$  BTE structures at the  $2\sigma$  level of the former set, further probing the limits of how accurately and precisely an  $r_e^{SE}$  structure can be determined by rotational spectroscopy with CCSD(T) corrections. Despite obtaining an  $r_e^{SE}$  structure for thiazole that is a substantial improvement over its previous determinations, the agreement found for some parameters is problematic compared to the outstanding agreement found for pyrimidine<sup>25</sup> or even thiophene.<sup>31</sup> Our analysis of the thiazole structure supports the conclusion first made from the thiophene structural analysis that the current methodology cannot completely overcome the proximity of atoms to the principal axes. Future investigations of other molecules with third-row atoms (Si, P, S, Cl, etc.), but without any atoms lying near a principal axis, would provide an opportunity to further explore and perhaps confirm this assertion. Interestingly, by comparison to the work on thiophene ( $C_{2\nu}$ ), this study may demonstrate that a dataset that includes as many as 24 isotopologues is insufficient to determine an  $r_e^{\text{SE}}$  structure for thiazole  $(C_s)$  at the same level of accuracy and precision that can be obtained for a molecule of comparable size but with fewer structural parameters. Whether or not this conjecture is valid could be tested by additional spectroscopy, but these measurements would require the chemical synthesis of multiple isotopically labeled thiazoles that is beyond the scope of this study.

The use of a large number of isotopologues in the experimental dataset and high-level computations results in converged parameters of thiazole with remarkably small statistical uncertainties. By many metrics, the high-level CCSD(T)/cc-pCV5Z structure is very good, but addressing the computed structure for very small contributions from a finite basis set, untreated correlation, relativistic effects, and the diagonal Born-Oppenheimer correction makes important, nonnegligible changes in the predicted structural parameters. These small changes are important for achieving agreement between the semi-experimental and theoretical structural parameters where the atoms involved are located far from a principal axis. An interesting result of the precision of both the  $r_e^{SE}$  and the BTE  $r_e$  structure is that a discrepancy between the semi-experimental and theoretical structural parameters is still apparent. They reveal that the classical difficulty in determining atom locations when close to an inertial axis, initially observed in substitution structures, cannot be easily overcome, even with 24 isotopologues and CCSD(T) calculations with a very large basis set. It is likely that for parameters involving atoms lying close to an inertial axis, the high-level theoretical calculations (BTE) are more reliable estimates of a molecular structure than the CCSD(T)-corrected  $r_e^{SE}$ , despite the general high precision and accuracy of this method.

### SUPPLEMENTARY MATERIAL

Computational output files, least-squares fitting output files for all isotopologues, data distribution plots for all non-standard isotopologues, detailed synthetic procedures for preparing deuterium-containing thiazoles along with their mass spectra, *xrefiteration* output, equations used to calculate determinable constants, and a table of determinable constants are provided in the supplementary material.

### **ACKNOWLEDGMENTS**

We gratefully acknowledge the National Science Foundation for the support of this project (Grant Nos. R.J.M. CHE-1664912, CHE-1954270, and J.F.S. CHE-1664325) and support for the shared mass spectrometry facility (Thermo Scientific Q Exactive Plus mass spectrometer, NIH 1S10 OD020022-1). We thank Michael McCarthy for the loan of an amplification-multiplication chain and the Harvey Spangler Award (to B.J.E.) for funding that supported the purchase of the corresponding detector.

### **DATA AVAILABILITY**

The data that support the findings of this study are available within the article and its supplementary material.

### **REFERENCES**

- <sup>1</sup>L. Bettendorff, "Thiamine," in *Handbook of Vitamins*, 5th ed., edited by J. Zempleni, J. W. Suttie, J. F. Gregory III, and P. J. Stover (CRC Press, 2014).
- <sup>2</sup>M. T. Chhabria, S. Patel, P. Modi, and P. S. Brahmkshatriya, "Thiazole: A review on chemistry, synthesis and therapeutic importance of its derivatives," Curr. Top. Med. Chem. 16, 2841 (2016).
- <sup>3</sup>B. A. McGuire, A. M. Burkhardt, S. Kalenskii, C. N. Shingledecker, A. J. Remijan, E. Herbst, and M. C. McCarthy, "Detection of the aromatic molecule benzonitrile (c- $C_6$ H $_5$ CN) in the interstellar medium," Science 359, 202–205 (2018).
- <sup>4</sup>M. C. McCarthy, K. L. K. Lee, R. A. Loomis, A. M. Burkhardt, C. N. Shingledecker, S. B. Charnley, M. A. Cordiner, E. Herbst, S. Kalenskii, E. R. Willis, C. Xue, A. J. Remijan, and B. A. McGuire, "Interstellar detection of the highly polar five-membered ring cyanocyclopentadiene," Nat. Astron. 5, 176–180 (2021).
- <sup>5</sup>B. A. McGuire, R. A. Loomis, A. M. Burkhardt, K. L. K. Lee, C. N. Shingledecker, S. B. Charnley, I. R. Cooke, M. A. Cordiner, E. Herbst, S. Kalenskii, M. A. Siebert, E. R. Willis, C. Xue, A. J. Remijan, and M. C. McCarthy, "Detection of two interstellar polycyclic aromatic hydrocarbons via spectral matched filtering," Science 371, 1265–1269 (2021).
- <sup>6</sup>See https://cdms.astro.uni-koeln.de/classic/molecules for the Cologne Database for Molecular Spectroscopy.
- <sup>7</sup>B. Bak, D. Christensen, L. Hansen-Nygaard, and J. Rastrup-Andersen, "Microwave spectrum and dipole moment of thiazole," J. Mol. Spectrosc. 9, 222–224 (1962).
- <sup>8</sup>L. Nygaard, E. Asmussen, J. H. Høg, R. C. Maheshwari, C. H. Nielsen, I. B. Petersen, J. Rastrup-Andersen, and G. O. Sørensen, "Microwave spectra of isotopic thiazoles. Molecular structure <sup>14</sup>N quadrupole coupling constants of thiazole," J. Mol. Struct. **8**, 225–233 (1971).
- <sup>9</sup>I. N. Bojesen, J. H. Høg, J. T. Nielsen, I. B. Petersen, and K. Schaumburg, "Preparation, mass and NMR spectra of some isotopic thiazoles," Acta Chem. Scand. **25**, 2739–2748 (1971).
- $^{10}\mathrm{J}.$  A. Braun and J. Metzger, "Isotopic synthesis of thiazole," Caplus An **411446**, 503–510 (1967).
- <sup>11</sup>P. Roussel and J. Metzger, "Synthesis and infrared spectral study of the deuteriothiazoles," Bull. Soc. Chim. Fr. 1962, 2075–2078.

- 12W. F. White, "Microwave spectra of some sulfur and nitrogen compounds," NASA Technical Note NASA TN D-7450, National Aeronautics and Space Administration, Washington, DC, 1974.
- <sup>13</sup>J. Wiese and D. H. Sutter, "The rotational Zeeman effect of thiazole and isothiazole," Z. Naturforsch., A 35, 712-722 (1980).
- <sup>14</sup>U. Kretschmer and H. Dreizler, <sup>«33</sup>S nuclear hyperfine structure in the rotational spectrum of thiazole," Z. Naturforsch., A 48, 1219–1222 (1993).
   <sup>15</sup>B. P. van Eijck, "Reformulation of quartic centrifugal distortion Hamiltonian,"
- J. Mol. Spectrosc. 53, 246-249 (1974).
- <sup>16</sup>F. Hegelund, R. W. Larsen, and M. H. Palmer, "The vibrational spectrum of thiazole between 600 and 1400 cm<sup>-1</sup> revisited: A combined high-resolution infrared and theoretical study," J. Mol. Spectrosc. 244, 63-78 (2007).
- <sup>17</sup>S. F. Bone, B. A. Smart, H. Gierens, C. A. Morrison, P. T. Brain, and D. W. H. Rankin, "The molecular structure of thiazole, determined by the combined analysis of gas-phase electron diffraction (GED) data and rotational constants and by ab initio calculations," Phys. Chem. Chem. Phys. 1, 2421-2426 (1999).
- <sup>18</sup>E. Penocchio, M. Mendolicchio, N. Tasinato, and V. Barone, "Structural features of the carbon-sulfur chemical bond: A semi-experimental perspective," Can. J. Chem. 94, 1065-1076 (2016).
- <sup>19</sup>M. A. Zdanovskaia, B. J. Esselman, R. C. Woods, and R. J. McMahon, "The 130-370 GHz rotational spectrum of phenyl isocyanide (C<sub>6</sub>H<sub>5</sub>NC)," J. Chem. Phys. 151, 024301 (2019).
- <sup>20</sup>B. J. Esselman, B. K. Amberger, J. D. Shutter, M. A. Daane, J. F. Stanton, R. C. Woods, and R. J. McMahon, "Rotational spectroscopy of pyridazine and its isotopologs from 235-360 GHz: Equilibrium structure and vibrational satellites," J. Chem. Phys. 139, 224304 (2013).
- <sup>21</sup> Z. Kisiel, L. Pszczółkowski, B. J. Drouin, C. S. Brauer, S. Yu, J. C. Pearson, I. R. Medvedev, S. Fortman, and C. Neese, "Broadband rotational spectroscopy of acrylonitrile: Vibrational energies from perturbations," J. Mol. Spectrosc. 280, 134-144 (2012).
- <sup>22</sup>Z. Kisiel, L. Pszczółkowski, I. R. Medvedev, M. Winnewisser, F. C. De Lucia, and E. Herbst, "Rotational spectrum of trans-trans diethyl ether in the ground and three excited vibrational states," J. Mol. Spectrosc. 233, 231-243 (2005).
- <sup>23</sup>Z. Kisiel, "Assignment and Analysis of Complex Rotational Spectra," in Spectroscopy from Space, edited by J. Demaison, K. Sarka, and E. A. Cohen (Kluwer Academic Publishers: Dordrecht, 2001; pp. 91-106); http://www.ifpan. edu.pl/~kisiel/prospe.htm.
- <sup>24</sup>J. F. Stanton, L. Cheng, M. E. Harding, D. A. Matthews, and P. G. Szalay, "CFOUR, coupled-cluster techniques for computational chemistry," with contributions from A. A. Auer, R. J. Bartlett, U. Benedikt, C. Berger, D. E. Bernholdt, S. Blaschke, Y. J. Bomble, S. Burger, O. Christiansen, D. Datta, F. Engel, R. Faber, J. Greiner, M. Heckert, O. Heun, M. Hilgenberg, C. Huber, T.-C. Jagau, D. Jonsson, J. Jusélius, T. Kirsch, K. Klein, G. M. Kopper, W. J. Lauderdale, F. Lipparini, T. Metzroth, L. A. Mück, T. Nottoli, D. P. O'Neill, D. R. Price, E. Prochnow, C. Puzzarini, K. Ruud, F. Schiffmann, W. Schwalbach, C. Simmons, S. Stopkowicz, A. Tajti, J. Vázquez, F. Wang, J. D. Watts and the integral packages MOLECULE (J. Almlöf and P. R. Taylor), PROPS (P. R. Taylor), ABACUS (T. Helgaker, H. J. Aa. Jensen, P. Jørgensen, and J. Olsen), and ECP routines by A. V. Mitin and C. van Wüllen, http://www.cfour.de.
- <sup>25</sup>Z. N. Heim, B. K. Amberger, B. J. Esselman, J. F. Stanton, R. C. Woods, and R. J. McMahon, "Molecular structure determination: Equilibrium structure of pyrimidine  $(m\text{-}C_4H_4N_2)$  from rotational spectroscopy  $(r_e^{SE})$  and high-level ab initio calculation  $(r_e)$  agree within the uncertainty of experimental measurement," J. Chem. Phys. 152, 104303 (2020).
- <sup>26</sup> A. N. Owen, M. A. Zdanovskaia, B. J. Esselman, J. F. Stanton, R. C. Woods, and R. J. McMahon, "Semi-experimental equilibrium  $(r_e^{\text{SE}})$  and theoretical structures of pyridazine (o-C<sub>4</sub>H<sub>4</sub>N<sub>2</sub>)" (submitted).
- <sup>27</sup>M. J. Frisch, G. W. Trucks, H. B. Schlegel, G. E. Scuseria, M. A. Robb, J. R. Cheeseman, G. Scalmani, V. Barone, G. A. Petersson, H. Nakatsuji, X. Li, M. Caricato, A. V. Marenich, J. Bloino, B. G. Janesko, R. Gomperts, B. Mennucci, H. P. Hratchian, J. V. Ortiz, A. F. Izmaylov, J. L. Sonnenberg, D. Williams-Young, F. Ding, F. Lipparini, F. Egidi, J. Goings, B. Peng, A. Petrone, T. Henderson, D. Ranasinghe, V. G. Zakrzewski, J. Gao, N. Rega, G. Zheng, W. Liang, M. Hada, M.

- Ehara, K. Toyota, R. Fukuda, J. Hasegawa, M. Ishida, T. Nakajima, Y. Honda, O. Kitao, H. Nakai, T. Vreven, K. Throssell, J. A. Montgomery, Jr., J. E. Peralta, F. Ogliaro, M. J. Bearpark, J. J. Heyd, E. N. Brothers, K. N. Kudin, V. N. Staroverov, T. A. Keith, R. Kobayashi, J. Normand, K. Raghavachari, A. P. Rendell, J. C. Burant, S. S. Iyengar, J. Tomasi, M. Cossi, J. M. Millam, M. Klene, C. Adamo, R. Cammi, J. W. Ochterski, R. L. Martin, K. Morokuma, O. Farkas, J. B. Foresman, and D. J. Fox, Gaussian 16, Revision C.01, Gaussian, Inc., Wallingford, CT, 2016. <sup>28</sup>See http://www.webmo.net for WebMO Enterprise, version 19.0, WebMO LLC, Madison, WI, 2019; accessed August 2019.
- <sup>29</sup>B. J. Esselman, M. A. Zdanovskaia, T. K. Adkins, B. E. Billinghurst, J. Zhao, R. C. Woods, and R. J. McMahon, "Millimeter-wave and infrared spectroscopy of thiazole (c-C3H3NS) in its ground state and lowest-energy vibrationally excited states ( $\nu_{18}$ ,  $\nu_{17}$ , and  $\nu_{13}$ )," J. Mol. Spectrosc. 379, 111493
- $^{30}$ R. Venkatasubramanian and S. L. N. G. Krishnamachari, "Synthesis of (2-d)thiazole and (2-d)-oxazole and formation of pyrazine from reaction of oxazole," Indian J. Chem., Sect. B 29B, 562-563 (1990).
- <sup>31</sup> V. L. Orr, Y. Ichikawa, A. R. Patel, S. M. Kougias, K. Kobayashi, J. F. Stanton, B. J. Esselman, R. C. Woods, and R. J. McMahon, "Precise equilibrium structure determination of thiophene (c-C<sub>4</sub>H<sub>4</sub>S) by rotational spectroscopy—Structure of a five-membered heterocycle containing a third row atom," J. Chem. Phys. 154, 244310 (2021).
- $^{\bf 32}$  J. C. Kromann, J. H. Jensen, M. Kruszyk, M. Jessing, and M. Jørgensen, "Fast and accurate prediction of the regioselectivity of electrophilic aromatic substitution reactions," Chem. Sci. 9, 660-665 (2018).
- <sup>33</sup>V. Ji Ram, A. Sethi, M. Nath, and R. Pratap, "Five-membered heterocycles," in The Chemistry of Heterocycles, edited by V. Ji Ram, A. Sethi, M. Nath, and R. Pratap (Elsevier, 2019), Chap. 5, pp. 149-478.
- <sup>34</sup>J. V. Metzger, E. J. Vincent, J. Chouteau, and G. Mille, "Properties and reactions of thiazole," Chem. Heterocycl. Compd. 34, 5-164 (1979).
- 35 R. A. Coburn, J. M. Landesberg, D. S. Kemp, and R. A. Olofson, "An additionelimination mechanism for C-H/C-D exchange in thiazole," Tetrahedron 26, 685-692 (1970).
- <sup>36</sup>H. A. Staab, M.-T. Wu, A. Mannschreck, and G. Schwalbach, "H/D-austausch bei azolen und azolium-salzen," Tetrahedron Lett. 5, 845-848 (1964).
- <sup>37</sup>C. J. Moody and J. C. A. Hunt, "Synthesis of virenamide B, a cytotoxic thiazolecontaining peptide," J. Org. Chem. 64, 8715-8717 (1999).
- <sup>38</sup>D. Kikelj and U. Urleb, in Category 2, Hetarenes and Related Ring Systems, edited by E. Schaumann (Georg Thieme Verlag, Stuttgart, 2002), Vol. 11.
- 39 J. F. Arenas, J. Perez-Peña, and M. Gonzalez-Davila, "Vibrational spectra and thermodynamic properties of thiazole, 2-aminothiazole, 2-amino-[2H]thiazole and 2-amino-[2H2]-thiazole," Collect. Czech. Chem. Commun. 54, 28-41
- <sup>40</sup>J. Kraitchman, "Determination of molecular structure from microwave spectroscopic data," Am. J. Phys. 21, 17-24 (1953).
- <sup>41</sup>B. K. Amberger, B. J. Esselman, J. F. Stanton, R. C. Woods, and R. J. McMahon, "Precise equilibrium structure determination of hydrazoic acid (HN<sub>3</sub>) by millimeter-wave spectroscopy," J. Chem. Phys. 143, 104310 (2015).
- <sup>42</sup>C. Puzzarini, J. Bloino, N. Tasinato, and V. Barone, "Accuracy and interpretability: The devil and the holy grail. New routes across old boundaries in computational spectroscopy," Chem. Rev. 119, 8131-8191 (2019).
- 43 Y. J. Bomble, J. F. Stanton, M. Kállay, and J. Gauss, "Coupled-cluster methods including noniterative corrections for quadruple excitations," J. Chem. Phys. 123, 054101 (2005).
- <sup>44</sup>K. G. Dyall, "Interfacing relativistic and nonrelativistic methods. II. Investigation of a low-order approximation," J. Chem. Phys. 109, 4201-4208 (1998).
- <sup>45</sup>W. Liu and D. Peng, "Exact two-component Hamiltonians revisited," J. Chem. Phys. 131, 031104 (2009).
- $^{\mathbf{46}}$ L. Cheng and J. Gauss, "Analytic energy gradients for the spin-free exact twocomponent theory using an exact block diagonalization for the one-electron Dirac Hamiltonian," J. Chem. Phys. 135, 084114 (2011).
- <sup>47</sup>M. Born and K. Huang, *Dynamical Theory of Crystal Lattices* (Oxford University Press, 1954).